Towards a More General Many-objective Evolutionary Optimizer

Jesús Guillermo Falcón-Cardona$^{(\boxtimes)}$ and Carlos A. Coello Coello

Computer Science Department, CINVESTAV-IPN,
Av. IPN No. 2508, Col. San Pedro Zacatenco, 07300 México D.F., Mexico
jfalcon@computacion.cs.cinvestav.mx, ccoello@cs.cinvestav.mx

Abstract. Recently, it has been shown that the current Many-Objective Evolutionary Algorithms (MaOEAs) are overspecialized in solving certain benchmark problems. This overspecialization is due to a high correlation between the Pareto fronts of the test problems with the convex weight vectors commonly used by MaOEAs. The main consequence of such overspecialization is the inability of these MaOEAs to solve the minus versions of well-known benchmarks (e.g., the DTLZ^{-1} test suite). In furtherance of avoiding this issue, we propose a novel steady-state MaOEA that does not require weight vectors and uses a density estimator based on the IGD$^+$ indicator. Moreover, a fast method to calculate the IGD$^+$ contributions is integrated in order to reduce the computational cost of the proposed approach, which is called IGD$^+$-MaOEA. Our proposed approach is compared with NSGA-III, MOEA/D, IGD$^+$-EMOA (the previous ones employ convex weight vectors) and SMS-EMOA on the test suites DTLZ and DTLZ^{-1}, using the hypervolume indicator. Our experimental results show that IGD$^+$-MaOEA is a more general optimizer than MaOEAs that need a set of convex weight vectors and it is competitive and less computational expensive than SMS-EMOA.

Keywords: Multi-objective optimization · Quality indicators
Density estimation

1 Introduction

In the scientific and industrial fields, there is a wide variety of problems that involve the simultaneous optimization of several, often conflicting, objective functions. These are the so-called multi-objective optimization problems (MOPs) which are mathematically defined as follows:

$$\min_{\boldsymbol{x} \in \Omega} \boldsymbol{F}(\boldsymbol{x}) = (f_1(\boldsymbol{x}), f_2(\boldsymbol{x}), \ldots, f_m(\boldsymbol{x}))^T \tag{1}$$

where $\boldsymbol{x}$ is the vector of decision variables, $\Omega \subseteq \mathbb{R}^n$ is the decision variable space and $\boldsymbol{F}(\boldsymbol{x})$ is the vector of $m(\geq 2)$ objective functions. The solution of an MOP is a set of solutions that represent the best possible trade-offs among the objectives, i.e., finding solutions in which an objective function cannot be improved without worsening another. The particular set that yields the optimal values is known as the Pareto Optimal Set ($\mathcal{P}^*$) and its image in the objective space is known as the Pareto Optimal Front ($\mathcal{PF}^*$).

Multi-Objective Evolutionary Algorithms (MOEAs) are population-based and gradient-free methods that have been successfully applied to solve MOPs [1]. For several years, MOEAs have adopted the Pareto dominance relation.[1] However, Pareto-based MOEAs does not perform properly when tackling MOPs having four or more objective functions, i.e., the so-called many-objective optimization problems (MaOPs) [2]. This behavior is due to the rapid increase of solutions preferred by the use of Pareto dominance which directly produces a dilution of the selection pressure. With the aim of properly regulating the selection pressure of a MOEA three main approaches have been considered for MaOPs: (1) to define new dominance relations (mainly based on relaxed forms of Pareto dominance), (2) decomposition of the MOP, and (3) indicator-based selection.

Many-Objective Evolutionary Algorithms (MaOEAs) based on decomposition and performance indicators[2] are the most popular alternatives in the current literature [2]. Most of the state-of-the-art MaOEAs employ a set of convex weight vectors. A vector $\boldsymbol{w} \in \mathbb{R}^m$ is a convex weight vector if $\sum_{i=1}^{m} w_i = 1$ and $w_i \geq 0$ for all $i = 1, \ldots, m$. These weight vectors lie on an $(m-1)$-simplex and are used by MaOEAs as search directions [3], reference points [4,5] or as part of an indicator's definition [6]. However, in 2017, Ishibuchi $et\ al.$ [7] empirically showed that the use of convex weight vectors overspecializes MaOEAs on MOPs whose Pareto fronts are strongly correlated to the simplex formed by the weight vectors.

In this paper, we propose a steady-state MaOEA that uses Pareto dominance as its main selection criterion and a density estimator based on the Inverted Generational Distance plus (IGD$^+$) indicator. The proposed approach, called IGD$^+$-MaOEA, does not require a set of convex weight vectors in any of its mechanisms in furtherance of avoiding the previously indicated overspecialization. Furthermore, a fast IGD$^+$ contribution computation method is integrated into the proposed approach to reduce its computational cost.

The remainder of this paper is organized as follows. Section 2 presents an overview of some state-of-the-art MaOEAs. The detailed description of our proposal is outlined in Sect. 3. Our experimental results are provided in Sect. 4. Finally, Sect. 5 presents our conclusions and some possible paths for future work.

---

[1] Given two solutions $\boldsymbol{u}, \boldsymbol{v} \in \mathbb{R}^m$, $\boldsymbol{u}$ $dominates$ $\boldsymbol{v}$ (denoted as $\boldsymbol{u} \prec \boldsymbol{v}$), if and only if $u_i \leq v_i$ for all $i = 1, \ldots, m$ and there exists at least an index $j \in \{1, \ldots, m\}$ such that $u_i < v_i$. In case $u_i \leq v_i$ for all $i = 1, \ldots, m$, $\boldsymbol{u}$ is said to $weakly\ dominate$ $\boldsymbol{v}$ (denoted as $\boldsymbol{u} \preceq \boldsymbol{v}$).

[2] A unary performance indicator I is a function that assigns a real value to a set of m-dimensional vectors.

2   Previous Related Work

The MOEA based on Decomposition (MOEA/D) [3] transforms an MOP into as many single-objective optimization problems as weight vectors there are, through a scalarizing function. For each weight vector $\boldsymbol{w}^i$, MOEA/D defines a neighborhood of size T, i.e., it finds the T nearest solutions to $\boldsymbol{w}^i$, using Euclidean distances. Using this neighborhood structure, MOEA/D tries to optimize the scalarizing functions at each generation simultaneously. Hence, the aim is to find the intersections between the Pareto front and the weight vectors according to the value of the scalarizing function.

Deb *et al.* [4] proposed the Nondominated Sorting Genetic Algorithm III (NSGA-III). NSGA-III uses a $(\mu + \lambda)$ selection scheme, i.e., using a population of μ potential parents produces, at each generation, λ offspring. Then, the union set of parents and offspring is classified using the nondominated sorting method [8] that creates a set of disjoint ranks $R_1, R_2, \ldots, R_k$, using Pareto dominance. Ranks are added into the next population until one of them (e.g., R_j) makes the population size to be larger than μ. Hence, some solutions have to be deleted from R_j using a density estimator that employs a set of convex weight vectors to define a niche count per weight vector. Solutions from the most crowded regions are deleted until the desired population size is achieved.

In 2016, Manoatl and Coello [5] introduced the IGD^+-Evolutionary Multi-Objective Algorithm (IGD^+-EMOA) that is an indicator-based MaOEA. They defined an environmental selection mechanism on the transformation of an MOP into a Linear Assignment Problem, using the IGD^+ indicator. As IGD^+ needs a reference set, the authors proposed to use a set of weight vectors that try to approximate the Pareto front geometry employing Lamé Superspheres. However, by doing this, only smooth concave or convex geometries can be appropriately approximated. Consequently, IGD^+-EMOA has difficulties to solve MOPs having highly irregular Pareto fronts, namely disconnected and degenerated.

The $\mathcal{S}$-Metric Selection Evolutionary Multi-Objective Algorithm (SMS-EMOA) [9] is a steady-state version of the NSGA-II [8] but it implements a density estimator based on the hypervolume (HV) indicator. Due to this HV-based density estimator, SMS-EMOA increases selection pressure and drives the population to the maximization of the HV, which is directly related to finding Pareto optimal solutions [10]. Moreover, SMS-EMOA does not rely on convex weight vectors. However, its main drawback is the high computational cost associated to the computation of the individual HV contributions when the number of objective functions is greater than three, which makes its use prohibitive in MaOPs.

3   Our Proposed Approach

Ishibuchi *et al.* [11] proposed the IGD^+ indicator as an improved version of the Inverted Generational Distance (IGD) indicator [1]. The main difference between

IGD$^+$ and IGD is that the former is weakly Pareto-compliant[3] while the latter is Pareto non-compliant. Mathematically, given an approximation to the Pareto front $\mathcal{A}$ and a reference set denoted as $\mathcal{Z}$, IGD$^+$ is defined as follows (we assume minimization):

$$\text{IGD}^+(\mathcal{A}, \mathcal{Z}) = \frac{1}{|\mathcal{Z}|} \sum_{z \in \mathcal{Z}} \min_{a \in \mathcal{A}} d^+(\boldsymbol{a}, \boldsymbol{z}), \tag{2}$$

where $d^+(\boldsymbol{a}, \boldsymbol{z}) = \sqrt{\sum_{k=1}^{m}[\max(a_k - z_k, 0)]^2}$. IGD$^+$ measures the average distance from each reference vector to the nearest dominated region related to an element in $\mathcal{A}$. The aim is to minimize the value of IGD$^+$. If IGD$^+(\mathcal{A}, \mathcal{Z}) = 0$, it implies that $\mathcal{A} = \mathcal{Z}$; else if the value is greater than zero, IGD$^+$ intends to determine how different are both sets.

The contribution C of a solution $\boldsymbol{a} \in \mathcal{A}$ to IGD$^+$, is defined as follows:

$$C(\boldsymbol{a}, \mathcal{A}, \mathcal{Z}) = |\text{IGD}^+(\mathcal{A}, \mathcal{Z}) - \text{IGD}^+(\mathcal{A} \setminus \{\boldsymbol{a}\}, \boldsymbol{Z})|. \tag{3}$$

Clearly, the computational cost of calculating the contribution of a single solution is $\Theta(mNM)$, where $|\mathcal{A}| = N$ and $|\mathcal{Z}| = M$. Based on Eq. (3), our proposed IGD$^+$-based density estimator (IGD$^+$-DE) aims to delete from $\mathcal{A}$ the solution having the minimum contribution. The total runtime of IGD$^+$-DE is $\Theta(mN^2M)$ which is too expensive. In furtherance of reducing this computational cost, in the next section we propose a method based on memoization to achieve $\Theta(mNM)$ time for the full IGD$^+$-DE procedure.

3.1   Fast IGD$^+$ Contribution

IGD$^+$ in Eq. (2) is basically composed by $|\mathcal{Z}|$ minimum d^+ values, where each one is related to a solution, not necessarily different, in $\mathcal{A}$. If $\boldsymbol{a} \in \mathcal{A}$ is related to one or more elements in $\mathcal{Z}$, it is called *contributing solution*; otherwise, it is called *noncontributing solution*. It is worth noting that the IGD$^+$ contribution of the latter is zero, and, thus, IGD$^+$-DE deletes it first. Algorithm 1, proposed by Falcón-Cardona and Coello [12], stores in a memoization structure, for each $\boldsymbol{z} \in \mathcal{Z}$, the two smallest d^+ values and the corresponding pointers to the solutions in $\mathcal{A}$ (see Fig. 1) when IGD$^+(\mathcal{A}, \mathcal{Z})$ is computed in line 2. For each $\boldsymbol{a} \in \mathcal{A}$, the nested for-loops of lines 4–15 compute $\psi = \text{IGD}^+(\mathcal{A} \setminus \{\boldsymbol{a}\}, \mathcal{Z})$. For this purpose, the algorithm takes advantage of the memoization structure. If $\boldsymbol{a}$ is related to one or more minimum d^+ values, then the second best value is added to ψ; otherwise, the minimum d^+ is added. At the end, $C(\boldsymbol{a}, \mathcal{A}, \mathcal{Z}) = |\text{IGD}^+(\mathcal{A}, \mathcal{Z}) - \psi|$ is assigned to C_i. Consequently, the total runtime of Algorithm 1 is $\Theta(mNM) + \Theta(mNM) = \Theta(mNM)$.

When this method is integrated into IGD$^+$-DE, its overall cost goes from $\Theta(mN^2M)$ to $\Theta(mNM)$. The cost of calculating all the IGD$^+$ contributions is $\Theta(mNM)$ and it takes $\Theta(M)$ finding the minimum contribution, thus, $\Theta(mNM) + \Theta(M) = \Theta(mNM)$ is the runtime of IGD$^+$-DE.

---

[3] Let A and B be two non-empty sets of m-dimensional vectors and let I be a unary indicator. I is weakly Pareto-compliant if and only if A weakly dominates B implies $I(A) \leq I(B)$ (assuming minimization of I).
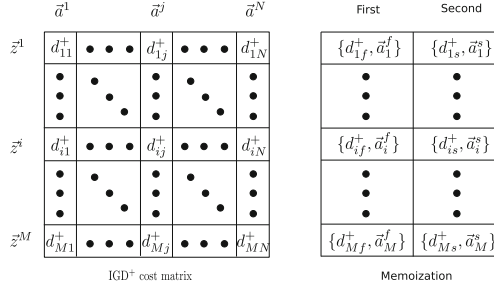
Fig. 1. IGD^+ cost matrix and the memoization structure. Each row of the memoization structure stores the two smalles d^+ values and the corresponding pointers to the related solutions.

Algorithm 1. Fast IGD^+ Contribution

Require: Approximation set $\mathcal{A}$ of size N; Reference set $\mathcal{Z}$ of size M
Ensure: Vector $C = (C_i)_{i=1,\ldots,N}$ of IGD^+ contributions
1: $Memoization \leftarrow \emptyset$
2: $total \leftarrow IGD^+(\mathcal{A}, \mathcal{Z}, Memoization)$
3: $\forall i \in \{1, \ldots, |\mathcal{A}|\}, C_i \leftarrow 0$
4: **for** $i = 1$ to N **do**
5:     $\psi \leftarrow 0$
6:     **for** $j = 1$ to M **do**
7:         **if** $Memoization[j].\boldsymbol{a}_j^f = \boldsymbol{a}^i$ **then**
8:             $\psi \leftarrow \psi + Memoization[j].d_{js}^+$
9:         **else**
10:            $\psi \leftarrow \psi + Memoization[j].d_{jf}^+$
11:        **end if**
12:    **end for**
13:    $\psi \leftarrow \psi/N$
14:    $C_i \leftarrow |total - \psi|$
15: **end for**
16: **return** C

3.2 IGD^+-MaOEA

IGD^+-MaOEA is a steady-state MOEA similar to SMS-EMOA [9]. However, instead of using HV contributions, this approach uses IGD^+-DE. Algorithm 2 describes the general framework of IGD^+-MaOEA, where the main loop is presented in lines 2 to 13. First, a new solution q is generated by variation operators.[4] q is added to P to create the temporary population Q which is ranked by the nondominated sorting method in line 5. If the layer R_k has more than one solution, then IGD^+-DE is executed in line 7, using Algorithm 1 where the set of nondominated solutions R_1 performs as the reference set $\mathcal{Z}$. In case $|R_k| = 1$, the sole solution of R_k is deleted. For both cases, $\boldsymbol{u}_{\text{worst}}$ denotes the solution to be deleted. In line 12, the population for the next generation is set. At the end of the evolutionary process, the current population P is returned.

---

[4] Simulated binary crossover (SBX) and polynomial-based mutation operators are employed [8].

Algorithm 2. IGD$^+$-MaOEA general framework

Require: No special parameters needed
Ensure: Approximation to the Pareto front
1: Randomly initialize population P
2: **while** stopping criterion is not fulfilled **do**
3:     $q \leftarrow Variation(P)$
4:     $Q \leftarrow P \cup \{q\}$
5:     $\{R_1, \ldots, R_k\} \leftarrow NondominatedSorting(Q)$
6:     **if** $|R_k| > 1$ **then**
7:         $C \leftarrow \text{IGD}^+\text{DE}(\mathcal{A} = R_k, \mathcal{Z} = R_1)$
8:         Let $\boldsymbol{u}_{\text{worst}}$ be the solution with the minimum IGD$^+$ contribution in C
9:     **else**
10:         Let $\boldsymbol{u}_{\text{worst}}$ be the sole solution in R_k
11:     **end if**
12:     $P \leftarrow Q \setminus \{\boldsymbol{u}_{\text{worst}}\}$
13: **end while**
14: **return** P

---

4   Experimental Results

In order to assess the performance of IGD$^+$-MaOEA[5], we used the Deb-Thiele-Laumanns-Zitzler (DTLZ) test suite and its minus version, DTLZ^{-1} proposed by Ishibuchi *et al.* [7] adopting $m = 3, 4, 5, 6, 7$ objective functions. For all DTLZ and DTLZ^{-1} instances, $n = m + K - 1$, where K is set to 5 for DTLZ1, 10 for DTLZ2-6 and 20 for DTLZ7 [1]. The values of K apply to the corresponding minus problems. The purpose of using DTLZ^{-1} is to show that IGD$^+$-MaOEA is more general than traditional MaOEAs based on the use of convex weight vectors. We compared IGD$^+$-MaOEA with respect to NSGA-III[6], MOEA/D[7], IGD$^+$-EMOA[8] and SMS-EMOA[9] (the latter for only MOPs having 3 and 4 objective functions due to its high computational cost). Results were compared using the hypervolume indicator, using the following reference points: $(1, 1, \ldots, 1)$ for DTLZ1/DTLZ1^{-1}, $(1, 1, \ldots, 1, 21)$ for DTLZ7/DTLZ7^{-1} and $(2, 2, \ldots, 2)$ for the remaining MOPs.

4.1   Parameters Settings

Since our approach and all the considered MaOEAs are genetic algorithms that use SBX and PBX, we set the crossover probability (P_c), crossover distribution index (N_c), mutation probability (P_m) and the mutation distribution index (N_m) as follows. For MOPs having 3 objective functions $P_c = 0.9$ and $N_c = 20$, while for MaOPs, $P_c = 1.0$ and $N_c = 30$. In all cases, $P_m = 1/n$, where n is the number

---

[5] The source code of IGD$^+$-MaOEA is available at http://computacion.cs.cinvestav.mx/~jfalcon/IGD+-MOEA.html.

[6] We used the implementation available at: http://web.ntnu.edu.tw/~tcchiang/publications/nsga3cpp/nsga3cpp.htm.

[7] We used the implementation available at: http://dces.essex.ac.uk/staff/zhang/webofmoead.htm.

[8] The source code was provided by its author, Edgar Manoatl Lopez.

[9] We employed the implementation available at jMetal 4.5.

of decision variables and $N_m = 20$. Table 1 shows the population size, objective function evaluations (employed as our stopping criterion) and the parameter H for the generation of the set of convex weight vectors described in [3]. The population size N is equal to the number of weight vectors, i.e., $N = C_{m-1}^{H+m-1}$. In all cases, the neighborhood size T of MOEA/D is set to 20.

Table 1. Common parameters settings

Objectives	3	4	5	6	7
Population size (N)	120	120	126	126	210
Objective function evaluations $(\times 10^3)$	50	60	70	80	90
Weight-vector partitions (H)	14	7	5	4	4

4.2 Comparison with MaOEAs Based on Convex Weight Vectors

Tables 3 and 4 show the average HV and the standard deviation (in parentheses) obtained by all the algorithms compared. The two best values among the MaOEAs are emphasized in grayscale, where the darker tone corresponds to the best value. Aiming to have statistical confidence of the results, we performed a one-tailed Wilcoxon test using a significance level of 0.05. Based on the Wilcoxon test, the symbol # is placed when IGD$^+$-MaOEA performs better than other MaOEA in a statistically significant way.

Regarding the original DTLZ problems, in Table 3 it is shown that IGD$^+$-MaOEA achieves the best performance in 9 out of 35 problems. Our proposed approach obtained the best HV values in DTLZ3, DTLZ5 and DTLZ6. For DTLZ7, IGD$^+$-MaOEA obtained the second best value when using from 5 to 7 objective functions. Regarding DTLZ1, DTLZ2 and DTLZ4, our proposed approach never obtained the first or the second best HV values among the compared MaOEAs in a statistically significant manner. Nevertheless, it is worth noting that numerically, the differences in all cases are minimal. On the other hand, NSGA-III obtained the best HV values in 7 of the 35 instances, being the best in DTLZ1 and DTLZ7. Overall, IGD$^+$-EMOA obtained the worst place in the performance rank because it only produced the best HV values only in 2 instances. Hence, we conclude that IGD$^+$-MaOEA outperforms MOEA/D and IGD$^+$-EMOA and is competitive with respect to NSGA-III.

Table 2. Average runtimes (in seconds) of IGD$^+$-MaOEA and SMS-EMOA on the DTLZ and DTLZ^{-1} test suites using 3 objective functions.

MaOEa	Type	DTLZ1	DTLZ2	DTLZ3	DTLZ4	DTLZ5	DTLZ6	DTLZ7
IGD$^+$-MaOEA	Original	55.87 s	81.66 s	42.44 s	72.80 s	54.92 s	65.31 s	76.26 s
	Minus	78.45 s	91.74 s	68.86 s	92.13 s	93.18 s	102.94 s	81.92 s
SMS-EMOA	Original	963.43 s	2144.43 s	359.28 s	1648.35 s	995.15 s	1944.93 s	1785.38 s
	Minus	1453.27 s	1868.63 s	1125.25 s	1906.52 s	1947.56 s	1950.85 s	1364.88 s

Table 3. Hypervolume results for the compared MOEAs on the DTLZ problems. We show the mean and standard deviations (in paretheses). The two best values are shown in gray scale, where the darker tone corresponds to the best value. The symbol # is placed when IGD⁺-MaOEA performs better in a statistically significant way.

MOP	Dim.	IGD$^+$-MaOEA	IGD$^+$-EMOA	NSGA-III	MOEA/D	SMS-EMOA
DTLZ1	3	9.664790e-01 (2.049666e-03)	9.740508e-01 (4.467021e-04)	9.741141e-01 (3.120293e-04)	9.740945e-01 (2.619649e-04)	9.745172e-01 (5.241259e-05)
	4	9.846496e-01 (2.656403e-03)	9.943998e-01 (9.261547e-05)	9.942231e-01 (8.570576e-04)	9.944018e-01 (6.220464e-05)	9.946409e-01 (2.134463e-05)
	5	9.881899e-01 (3.232379e-03)	9.943585e-01 (2.338311e-02)	9.986867e-01 (3.379577e-05)	9.986355e-01 (3.735697e-05)	
	6	9.906617e-01 (2.651917e-03)	9.035094e-01# (7.491169e-02)	9.996492e-01 (2.587221e-05)	9.996231e-01 (1.535746e-05)	
	7	9.948828e-01 (1.318848e-03)	9.264419e-01# (6.287378e-02)	9.999224e-01 (7.339504e-06)	9.998569e-01 (2.567104e-05)	
DTLZ2	3	7.420261e+00 (1.353052e-03)	7.421843e+00 (1.327349e-04)	7.421572e+00 (6.064709e-04)	7.421715e+00 (1.372809e-04)	7.431551e+00 (5.463841e-05)
	4	1.556161e+01 (2.748489e-03)	1.556734e+01 (4.007277e-04)	1.556646e+01 (6.681701e-04)	1.556718e+01 (2.213968e-04)	1.558874e+01 (6.349012e-05)
	5	3.166574e+01 (5.201361e-03)	3.166818e+01 (3.831826e-04)	3.166721e+01 (6.548007e-04)	3.166781e+01 (5.129480e-04)	
	6	6.373545e+01 (5.321646e-03)	6.182623e+01 (4.486397e+00)	6.373806e+01 (1.136133e-03)	6.373808e+01 (6.532194e-04)	
	7	1.278044e+02 (5.835291e-03)	1.117158e+02+ (1.213189e+01)	1.278161e+02 (1.524540e-03)	1.278230e+02 (4.937498e-04)	
DTLZ3	3	7.304310e+00 (5.416726e-01)	5.978405e+00# (2.296587e+00)	6.762070e+00# (1.512456e+00)	7.191410e+00# (9.234976e-01)	7.116381e+00# (1.038033e+00)
	4	1.554332e+01 (1.357241e-02)	1.553667e+01 (2.805291e-02)	1.426614e+01# (3.337968e+00)	1.525936e+01# (9.041126e-01)	1.557833e+01 (4.705930e-03)
	5	3.165020e+01 (9.384670e-03)	3.165404e+01 (6.820552e-03)	2.926244e+01# (5.291705e+00)	2.921654e+01# (6.617692e+00)	
	6	6.371498e+01 (1.113938e-02)	5.883028e+01# (5.646345e+00)	5.837271e+01# (1.552667e+01)	5.395689e+01# (1.319237e+01)	
	7	1.277759e+02 (1.177247e-02)	1.178341e+02# (3.658990e+00)	1.164877e+02# (2.147719e+01)	1.086977e+02# (2.778728e+01)	
DTLZ4	3	6.874113e+00 (7.238869e-01)	7.037545e+00 (7.189670e-01)	7.218780e+00 (4.062937e-01)	7.421636e+00 (1.147608e-04)	6.960992e+00 (5.030399e-01)
	4	1.495718e+01 (1.406114e+00)	1.491851e+01 (1.029726e+00)	1.540943e+01 (3.164949e-01)	1.556707e+01 (2.297960e-04)	1.506728e+01 (6.892799e-01)
	5	3.141161e+01 (5.091958e-01)	3.011363e+01# (1.320577e+00)	3.163040e+01 (1.455720e-01)	3.166733e+01 (4.792449e-04)	
	6	6.342094e+01 (8.053848e-01)	6.220439e+01# (4.109418e-01)	6.374155e+01# (5.870500e-04)	6.373585e+01 (1.078543e-03)	
	7	1.276686e+02 (5.342428e-01)	1.268979e+02# (4.641205e-01)	1.278235e+02 (5.765414e-04)	1.278246e+02 (3.325992e-04)	
DTLZ5	3	6.103250e+00 (3.206747e-04)	4.126358e+00# (1.356638e-01)	6.086240e+00# (3.462620e-03)	6.046024e+00# (2.227008e-04)	6.105419e+00 (1.265596e-05)
	4	1.195066e+01 (1.060364e-02)	8.053758e+00# (6.181680e-02)	1.176583e+01# (3.990838e-02)	1.187250e+01# (4.856384e-03)	1.200938e+01 (7.506854e-04)
	5	2.352758e+01 (5.631168e-02)	1.617222e+01# (1.916164e-01)	2.162912e+01# (9.476133e-01)	2.328373e+01# (1.640165e-02)	
	6	4.655654e+01 (1.477530e-01)	3.216498e+01# (2.350120e-01)	4.222308e+01# (1.270959e+00)	4.584961e+01# (4.179642e-02)	
	7	9.259723e+01 (2.885851e-01)	6.433872e+01# (6.900391e-01)	8.421920e+01# (2.089834e+00)	9.094108e+01# (1.339743e-01)	
DTLZ6	3	5.822452e+00 (9.468474e-02)	5.524093e+00# (8.062048e-01)	5.755154e+00# (7.832234e-02)	5.774939e+00# (8.361881e-02)	5.838678e+00 (7.196085e-02)
	4	1.141949e+01 (1.435037e-01)	9.520791e+00# (5.465663e-01)	5.969793e+00# (6.529944e-01)	1.136532e+01# (1.519071e-01)	1.112687e+01# (1.725538e-01)
	5	2.243194e+01 (2.205059e-01)	1.230783e-02# (1.960431e-02)	6.433325e+00# (1.002102e-01)	2.217372e+01# (3.778954e-01)	
	6	4.395244e+01 (4.872918e-01)	6.039732e+00# (1.208422e+01)	3.872393e+00# (7.548978e-01)	4.349163e+01# (5.731473e-01)	
	7	8.562322e+01 (8.346399e-01)	3.737526e+01# (3.051737e+01)	7.781012e+01# (2.442098e-00)	8.668146e+01 (1.610733e+00)	
DTLZ7	3	1.613138e+01 (1.102308e-01)	1.571995e+01# (7.026627e-02)	1.631926e+01 (1.253568e-02)	1.620770e+01 (1.240925e-01)	1.637100e+01 (7.629934e-02)
	4	1.435812e+01 (1.541455e-01)	1.364183e+01# (1.305431e-01)	1.462787e+01 (3.713300e-02)	1.406944e+01# (5.544544e-02)	1.483349e+01 (1.533320e-01)
	5	1.221977e+01 (5.193563e-01)	1.133320e+01# (1.223979e-01)	1.284401e+01 (3.182259e-02)	6.515913e+00# (1.170945e+00)	
	6	1.035596e+01 (4.758743e-01)	9.287520e+00# (9.704494e-02)	1.082465e+01 (7.434508e-02)	1.366732e+00# (1.894512e+00)	
	7	8.804845e+00 (3.468746e-01)	7.339032e+00# (9.787487e-02)	8.942419e+00 (5.155349e-02)	1.089167e-01# (1.867035e-01)	

Table 4. Hypervolume results for the compared MOEAs on the DTLZ^{-1} problems. We show the mean and standard deviations (in paretheses). The two best values are shown in gray scale, where the darker tone corresponds to the best value. The symbol # is placed when IGD^{+}-MaOEA performs better in a statistically significant way.

MOP	Dim.	IGD^{+}-MaOEA	IGD^{+}-EMOA	NSGA-III	MOEA/D	SMS-EMOA
DTLZ1^{-1}	3	2.264909e+07 (8.207717e+04)	1.140466e+07# (1.217933e+06)	2.044422e+07# (2.230718e+05)	1.708422e+07# (2.776295e+05)	1.640482e+07# (1.253694e+06)
	4	1.663320e+09 (4.001511e+07)	3.783933e+07# (1.747066e+07)	6.137596e+08# (8.114743e+07)	3.671230e+08# (8.437648e+07)	1.176107e+09# (1.162071e+08)
	5	6.119188e+10 (4.760735e+09)	3.145584e+06# (6.453973e+06)	1.653440e+10# (7.395153e+09)	1.275157e+10# (5.929635e+09)	
	6	1.040799e+12 (2.723386e+11)	5.143618e+05# (1.818714e+06)	3.525438e+11# (1.554685e+11)	6.835890e+10# (4.577981e+10)	
	7	1.879388e+13 (7.487935e+12)	3.352615e+05# (1.083160e+06)	5.717044e+12# (2.906156e+12)	5.582247e+11# (9.246709e+11)	
DTLZ2^{-1}	3	1.210884e+02 (9.009171e-01)	9.369690e+01# (5.010715e+00)	1.226427e+02 (4.332124e-01)	1.241646e+02 (1.767939e-01)	1.261046e+02 (1.456397e-02)
	4	4.674859e+02 (6.158074e+00)	6.908303e+01# (2.593222e-01)	4.670265e+02# (5.036135e+00)	4.782322e+02 (3.762262e-01)	5.109249e+02 (4.731194e-01)
	5	1.655899e+03 (3.942682e+01)	1.817170e+02# (2.352582e+00)	1.529187e+03# (3.829295e+01)	1.570781e+03# (5.466206e+00)	
	6	5.470358e+03 (1.134490e+02)	4.572952e+02# (8.088396e+00)	4.188435e+03# (3.496415e+02)	3.701069e+03# (1.866271e+01)	
	7	1.926684e+04 (4.521928e+02)	1.187017e+03# (1.260695e+01)	1.321225e+04# (1.030901e+03)	1.320162e+04# (6.203137e+01)	
DTLZ3^{-1}	3	5.017451e+09 (1.676399e+07)	3.163373e+09# (3.448716e+08)	4.769399e+09# (4.395958e+07)	4.788299e+09# (5.251105e+07)	3.617983e+09# (1.229064e+08)
	4	5.016984e+12 (2.782494e+10)	1.858417e+11# (1.368270e+11)	3.421113e+12# (1.621812e+11)	3.382020e+12# (8.277136e+10)	2.942443e+12# (1.497601e+11)
	5	4.010397e+15 (5.491013e+13)	2.308672e+10# (5.932196e+10)	1.418461e+15# (2.265638e+14)	2.169617e+15# (3.559794e+13)	
	6	2.671524e+18 (7.441405e+16)	6.882907e+09# (2.710629e+10)	4.952138e+17# (1.783349e+17)	7.151722e+17# (2.068326e+16)	
	7	1.792722e+21 (4.730737e+19)	3.686677e+10# (1.841504e+11)	1.374261e+20# (6.319205e+19)	8.941855e+20# (5.275602e+19)	
DTLZ4^{-1}	3	1.232680e+02 (5.341538e-01)	8.745995e+01# (7.308267e+00)	1.231716e+02# (3.158586e-01)	1.241412e+02 (2.261829e-01)	1.261219e+02 (1.400665e-02)
	4	4.872739e+02 (2.714648e+00)	6.889884e+01# (2.509073e-01)	4.703987e+02# (3.758543e+00)	4.774396e+02 (2.932713e-01)	5.114649e+02 (3.829142e-01)
	5	1.751991e+03 (1.604473e+01)	1.667599e+02# (4.139344e+01)	1.532427e+03# (3.367009e+01)	1.577174e+03# (3.235047e+00)	
	6	5.844499e+03 (5.546305e+01)	4.266016e+02# (3.968221e+02)	4.188345e+03# (2.845836e+02)	3.654612e+03# (4.982487e+00)	
	7	2.024392e+04 (1.637229e+02)	2.470440e+02# (8.390175e+01)	1.311381e+04# (6.546800e+02)	1.295551e+04# (5.175739e+01)	
DTLZ5^{-1}	3	1.189566e+02 (1.131492e+00)	1.045511e+02# (2.925727e+00)	1.212729e+02 (4.506920e-01)	1.230132e+02 (1.173182e-01)	1.248782e+02 (1.400672e-02)
	4	4.524837e+02 (6.184888e+00)	1.458893e+02# (1.837707e+01)	4.617533e+02# (3.033948e+00)	4.737665e+02 (5.201724e-01)	5.067611e+02 (3.943537e-01)
	5	1.590424e+03 (3.260130e+01)	1.247849e+03# (7.727654e+01)	1.526551e+03# (4.186892e+01)	1.532378e+03# (6.612506e+00)	
	6	5.201281e+03 (1.024733e+02)	4.775094e+03# (8.471898e+02)	3.648377e+03# (3.589604e+02)	3.670455e+03# (1.117756e+01)	
	7	1.798605e+04 (3.438881e+02)	3.663675e+03# (2.075826e+03)	1.169538e+04# (9.150133e+02)	1.287945e+04# (5.086978e+01)	
DTLZ6^{-1}	3	1.277596e+03 (8.980299e+00)	5.926270e+02# (4.387564e+01)	1.281204e+03 (4.388455e+00)	1.290813e+03 (6.053013e-01)	1.307600e+03 (1.645502e+00)
	4	9.344785e+03 (1.172155e+02)	7.139870e+03# (1.364398e+02)	8.894185e+03# (9.665925e+01)	8.908490e+03# (7.411574e+00)	9.489564e+03 (6.321189e+01)
	5	5.967159e+04 (9.243485e+02)	4.054599e+03# (5.178149e+02)	4.774990e+04# (2.111510e+03)	5.337501e+04# (1.101944e+02)	
	6	3.401029e+05 (5.077651e+03)	2.826444e+04# (4.152159e+03)	1.871320e+05# (4.124992e+04)	1.611984e+05# (2.134698e+02)	
	7	2.037163e+06 (1.966308e+04)	6.996351e+04# (2.447352e+02)	6.943417e+05# (1.558202e+05)	1.227654e+06# (7.772613e+03)	
DTLZ7^{-1}	3	2.145249e+02 (5.714409e-01)	2.121154e+02# (5.197201e+00)	2.144482e+02 (1.844494e-02)	2.144785e+02 (3.401603e-03)	2.143458e+02# (2.207311e-04)
	4	5.142917e+02 (2.116147e+00)	4.945863e+02# (1.805875e+01)	5.130456e+02# (1.613943e+00)	5.083181e+02# (1.486713e+01)	5.142100e+02# (1.152841e+00)
	5	1.199552e+03 (5.112678e+00)	4.348046e+02# (6.886537e+01)	1.190442e+03# (4.159670e+00)	6.388549e+02# (5.254422e+01)	
	6	2.741875e+03 (1.509787e+01)	7.362027e+02# (1.136842e+02)	2.691994e+03# (7.841504e+00)	9.262902e+02# (3.468054e+00)	
	7	6.176946e+03 (1.308306e+01)	1.355104e+03# (3.306126e+02)	6.016129e+03# (2.260447e+01)	1.621765e+03# (1.220737e+02)	

Table 4 shows the statistical results for the $DTLZ^{-1}$ test suite. IGD^+-MaOEA is the best MaOEA in these problems because it presented the best HV values in 27 out of 35 instances. Its performance is more evident when tackling the instances having many objectives. In case of three-dimensional problems, it obtained the second best overall HV values, being SMS-EMOA the best optimizer. It is worth noticing that none of the MaOEAs that use convex weight vectors obtained the best HV value in any of the problems. This strongly evidences their overspecialization in MOPs whose Pareto fronts are closely related to the shape of an $(m-1)$-simplex. MOEA/D obtained the second place in 16 problems and NSGA-III in 15. IGD^+-EMOA is the worst MaOEA in these problems as it never obtained the best HV values nor the second best ones. Hence, it is evident that the strategy based on weight vectors for the construction of the IGD^+-EMOA's reference set has a negative impact on its performance. Moreover, based on the direct comparison between IGD^+-MaOEA and IGD^+-EMOA, the former can be considered as a better optimizer.

4.3   Comparison with SMS-EMOA

From Tables 3 and 4, it is clear that SMS-EMOA outperforms IGD^+-MaOEA in the DTLZ test suite and that both are competitive in the $DTLZ^{-1}$ instances. However, the aim of SMS-EMOA is to maximize HV and this indicator is being employed for comparison purposes which clearly favor this algorithm. Nevertheless, it is worth noting that the overall HV differences between both algorithms is not very significant. It is also worth highlighting that IGD^+-MaOEA generates similar distributions to those of SMS-EMOA. This is shown in Fig. 2 where
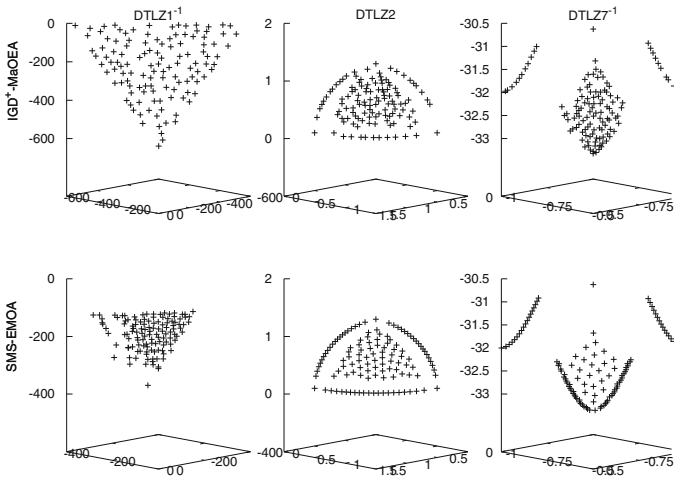

Fig. 2. Pareto fronts produced by IGD^+-MaOEA and SMS-EMOA for $DTLZ1^{-1}$, DTLZ2 and $DTLZ7^{-1}$ for 3 objective functions. Each front corresponds to the median HV values.

the Pareto fronts for DTLZ2 are similar. This distribution is due to the use of the set of nondominated solutions as the reference set in the IGD$^+$-DE algorithm. Hence, this kind of reference set is highly recommended to approximate the performance of HV-based MaOEAs using the IGD$^+$ indicator. Moreover, the average computational cost of IGD$^+$-MaOEA is significantly lower than that of SMS-EMOA. This claim is supported by the average runtimes shown in Table 2.

5   Conclusions and Future Work

In this paper, we have proposed a steady-state MaOEA, called IGD$^+$-MaOEA, that adopts an IGD$^+$-based density estimator and Pareto dominance as its main selection criterion. Moreover, a fast method to compute the IGD$^+$ contributions is employed in order to reduce the computational cost from $\Theta(mN^2M)$ to $\Theta(mNM)$, where m is the number of objective functions, N is the cardinality of the approximation set and M the size of the reference set. IGD$^+$-MaOEA does not adopt convex weight vectors in any of its mechanisms. In consequence, the performance of IGD$^+$-MaOEA does not strongly depend on the Pareto front shape. Our experimental results show that IGD$^+$-MaOEA is a more general multi-objective optimizer because its performance does not degrade when solving the DTLZ^{-1} test suite. In fact, IGD$^+$-MaOEA is competitive with NSGA-III and outperforms MOEA/D and IGD$^+$-EMOA in the original DTLZ test suite and it outpeforms these MaOEAs in all the DTLZ^{-1} problems. Moreover, we compared our approach with SMS-EMOA and our experimental results indicate that IGD$^+$-MaOEA performs similarly to the former, which makes it a remarkable approach to approximate the performance of HV-based MaOEAs. As part of our future work, we are interested in producing uniformly distributed solutions for both the DTLZ and DTLZ^{-1} test suites. Furthermore, we aim to improve the convergence results of IGD$^+$-MaOEA in the DTLZ test problems without worsening its performance on the DTLZ^{-1} instances.

References

1. Coello, C.A.C., Lamont, G.B., Van Veldhuizen, D.A.: Evolutionary Algorithms for Solving Multi-objective Problems, 2nd edn. Springer, New York (2007). https://doi.org/10.1007/978-0-387-36797-2. ISBN 978-0-387-33254-3
2. Ishibuchi, H., Tsukamoto, N., Nojima, Y.: Evolutionary many-objective optimization: a short review. In: 2008 Congress on Evolutionary Computation (CEC 2008), Hong Kong, pp. 2424–2431. IEEE Service Center, June 2008
3. Zhang, Q., Li, H.: MOEA/D: a multiobjective evolutionary algorithm based on decomposition. IEEE Trans. Evol. Comput. **11**(6), 712–731 (2007)
4. Deb, K., Jain, H.: An evolutionary many-objective optimization algorithm using reference-point-based nondominated sorting approach, part i: solving problems with box constraints. IEEE Trans. Evol. Comput. **18**(4), 577–601 (2014)
5. Lopez, E.M., Coello, C.A.C.: IGD$^+$-EMOA: a multi-objective evolutionary algorithm based on IGD$^+$. In: 2016 IEEE Congress on Evolutionary Computation (CEC 2016), Vancouver, Canada, 24–29 July 2016, pp. 999–1006. IEEE Press (2016). ISBN 978-1-5090-0623-9

6. Gómez, R.H., Coello, C.A.C.: Improved metaheuristic based on the $R2$ indicator for many-objective optimization. In: 2015 Genetic and Evolutionary Computation Conference (GECCO 2015), Madrid, Spain, July 11–15 2015, pp. 679–686. ACM Press (2015). ISBN 978-1-4503-3472-3

7. Ishibuchi, H., Setoguchi, Y., Masuda, H., Nojima, Y.: Performance of decomposition-based many-objective algorithms strongly depends on pareto front shapes. IEEE Trans. Evol. Comput. **21**(2), 169–190 (2017)

8. Deb, K., Pratap, A., Agarwal, S., Meyarivan, T.: A fast and elitist multiobjective genetic algorithm: NSGA-II. IEEE Trans. Evol. Comput. **6**(2), 182–197 (2002)

9. Beume, N., Naujoks, B., Emmerich, M.: SMS-EMOA: multiobjective selection based on dominated hypervolume. Eur. J. Oper. Res. **181**(3), 1653–1669 (2007)

10. Fleischer, M.: The measure of pareto optima applications to multi-objective meta-heuristics. In: Fonseca, C.M., Fleming, P.J., Zitzler, E., Thiele, L., Deb, K. (eds.) EMO 2003. LNCS, vol. 2632, pp. 519–533. Springer, Heidelberg (2003). https://doi.org/10.1007/3-540-36970-8_37

11. Ishibuchi, H., Masuda, H., Tanigaki, Y., Nojima, Y.: Modified distance calculation in generational distance and inverted generational distance. In: Gaspar-Cunha, A., Henggeler Antunes, C., Coello, C.C. (eds.) EMO 2015. LNCS, vol. 9019, pp. 110–125. Springer, Cham (2015). https://doi.org/10.1007/978-3-319-15892-1_8

12. Falcón-Cardona, J.G., Coello, C.A.C.: Multi-objective evolutionary hyper-heuristic based on multiple indicator-based density estimators. In: 2018 Genetic and Evolutionary Computation Conference (GECCO 2018), Kyoto, Japan, 15–19 July 2018. ACM Press (To be published)